PROCEEDINGS OF SPIE

SPIEDigitalLibrary.org/conference-proceedings-of-spie

Bi-encoded metasurfaces for the infrared spectral range

Micheal McLamb, Yanzeng Li, Victoria Stinson, Nuren Shuchi, Dustin Louisos, et al.

Micheal McLamb, Yanzeng Li, Victoria P. Stinson, Nuren Shuchi, Dustin Louisos, Tino Hofmann, "Bi-encoded metasurfaces for the infrared spectral range," Proc. SPIE 12417, Optical Components and Materials XX, 124170L (14 March 2023); doi: 10.1117/12.2661109



Event: SPIE OPTO, 2023, San Francisco, California, United States

Bi-encoded metasurfaces for the infrared spectral range

Micheal McLamb^a, Yanzeng Li^b, Victoria P. Stinson^a, Nuren Shuchi^a, Dustin Louisos^a, and Tino Hofmann^a

^aUniversity of North Carolina at Charlotte, 9201 University City Blvd., Charlotte, NC 28223, USA

^bThe University of Chicago, 929 E 57th St., Chicago, IL 60637, USA

ABSTRACT

Plasmonic metasurfaces composed of arrays of rectangular metallic bars are well known for their strong optical response in the infrared spectral range. In this study, we explore the polarization sensitivity of plasmonic metasurfaces for encoding information. The polarization-sensitive optical response depends strongly on the orientation of the metallic bars allowing the encoding of information into the metasurface. Here we demonstrate that a 2-dimensional polarization encoded metasurface can be obtained by using mask-less two-photon polymerization techniques. This novel approach for the fabrication of plasmonic metasurfaces enables the rapid prototyping and adaptation of polarization sensitive metasurfaces for the encoding of multiplexed images.

Keywords: Metasurface, infrared, polarization sensitive, two-photon polymerization

1. INTRODUCTION

Metamaterials describe a group of materials with properties that are not typically found in nature. Metamaterials are designed to manipulate phase, amplitude, and polarization of electromagnetic radiation by implementing an array of subwavelength components with arbitrary optical properties which eliminates the need for classically bulky optical systems.¹ Metasurfaces are a subset of metamaterials which eliminate the height dimension of metamaterials in favor of a simpler design permitting an easing of the precision of fabrication requirements. Plasmonic metasurfaces are composed of a metallic array of components that utilize the plasmonic resonances, known as surface plasmon polaritons, to manipulate the optical response of incoming electromagnetic radiation and have a wide field of applications.¹⁻³ A few examples of metasurface applications include beam steering, planar metalenses, holography, and narrow and broadband absorbers.^{1,2,4,5} Metasurfaces can be fabricated using many techniques, for example, electron beam lithography, focused ion beam milling, interference lithography, and nano-imprint lithography, to name a few. Two-photon polymerization has been established as a mask-less lithographic technique which allows the fabrication of metasurfaces.^{6,7}

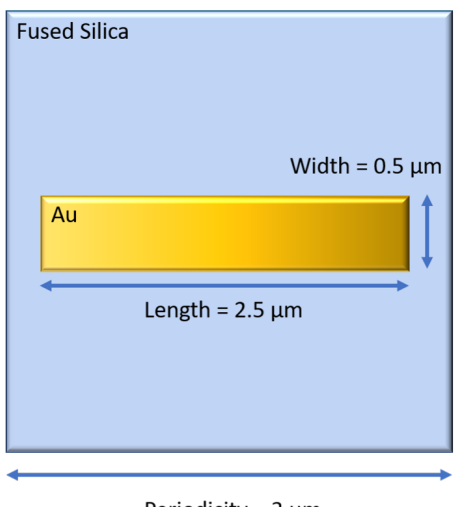
This work aims to show proof of concept for the encoding of information into a plasmonic metasurface fabricated using two-photon polymerization techniques. A metasurface composed of an arrangement of rectangular dipoles on a dielectric surface was designed and fabricated using two-photon polymerization with subsequent metallization. The metasurface was intended for use in the infrared spectrum. The reflected amplitude varies as a function of the linear polarization profile of the incident radiation to produce two distinct images. In this case, the image created by aligning the linear polarization along $0^{\circ} + (n \cdot 180^{\circ})$ of the dipole resonator produces the image of a "1" and aligning the linear polarization in angles of $45^{\circ} + (n \cdot 90^{\circ})$ forms the image of a "0" (where n = 0, 1, 2, ...). The fabrication of the metasurface uses a three-step technique that involves two-photon polymerization on a dielectric slap subsequently followed by a metallization step using electron-beam evaporation to form the metallic layer. The polymerized layer is then removed post-metallization with a lift-off technique leaving only the metallic dipoles on the dielectric layer. The encoding of metasurfaces through the polarization profile of incident radiation has applications in color display, information security, and anti-counterfeiting.³ This work will discuss the basic design principles, fabrication process, and experimental results for the rapid prototyping of an encoded polarization sensitive plasmonic metasurface.

Further author information: (Send correspondence to M.M.) M.M.: E-mail: mmclam10@uncc.edu, Telephone: 1 704 687 8020

Optical Components and Materials XX, edited by Shibin Jiang, Michel J. F. Digonnet, Proc. of SPIE Vol. 12417, 124170L © 2023 SPIE · 0277-786X · doi: 10.1117/12.2661109

2. DESIGN AND FABRICATION

2.1 Modeling



Periodicity = 3 μm

Figure 1. Represents the unit cell used in COMSOL Multiphysics. The bar resonator is composed of Au with 38 nm thickness which rests on a slab of fused silica with a square periodicity of 3 μ m. The length and width of the bar resonator is 2.5 μ m and 0.5 μ m respectively.

The dimensions and arrangement for the bar resonators were determined using finite element modeling (COMSOL). The resonators are arranged in a square lattice. The COMSOL calculations further require accurate knowledge of the constituents of the metasurface. The dielectric function of the fused silica substrate (Nanoscribe GmbH) was determined through spectroscopic ellipsometry in the range from 2 µm - 33 µm (IR-Vase, J.A. Woollam Co., Inc.).⁶ The Au optical properties are modeled with a single Drude oscillator with parameters $\rho_1 = (3.3 \pm 3 \times 10^{-7}) \times 10^{-6} \ \Omega/\text{cm}, \ \tau_1 = (18 \pm 1.13) \ fs.$ The boundaries of the unit cell were given periodic conditions to simulate an infinite array of resonators. The dimensional parameters of the unit cell were varied in order to determine the optimal conditions for a resonance to occur at a wavelength 6 µm when normally incident radiation is linearly polarized along the long axis and no resonance when polarized along the short axis of the resonator. The thickness of the Au layer was controlled at 38 nm, consistent with the measured thickness of the Au witness sample, with fused silica as the substrate, measured with spectroscopic ellipsometry. The optimal dimensions for a central reflectance maximum at $\lambda = 6 \, \mu \text{m}$ were found to be $l = 2.5 \, \mu \text{m}$, $w = 0.5 \, \mu \text{m}$, and p=3 µm. The unit cell can be viewed in Fig. 1. The results of the simulation were verified with experimental results which can be viewed in a previous publication.⁶ For brevity, the results of the simulation and experiment can be seen in Fig. 2. The reflectance map is used to determine what orientations should be used to create two distinct images. The green dots in Fig. 2 represent polarization states where the image of a "1" will appear, conversely, the red dots indicate states where the image of a "0" will appear. There is a secondary reflectance that is apparent at $\lambda = 9 \, \mu m$ which arises due to vibrational mode within the fused silica substrate.⁸ This reflectance maximum can be observed in all cases and thus can be determined to be polarization insensitive.

Once the optimal dimensions were determined, the resonators must be oriented in such a way as to construct an image when illuminated with the appropriate polarization. This was done by digitizing images of a "1" and "0" with pixels set at a periodicity of 3 µm using Matlab. Each image has two possible combinations, either "on" or "off" meaning there are four distinct combinations of images. These four sets of coordinates are superimposed on each other to create the locations and orientations of the bar resonators which can be seen in Fig. 3.

2.2 Two-photon polymerization

The total image coordinates obtained in Matlab are used to create a write file of the inverse of the desired metasurface which is fabricated by a commercial two-photon lithography system (Nanoscribe GmbH). The inverse

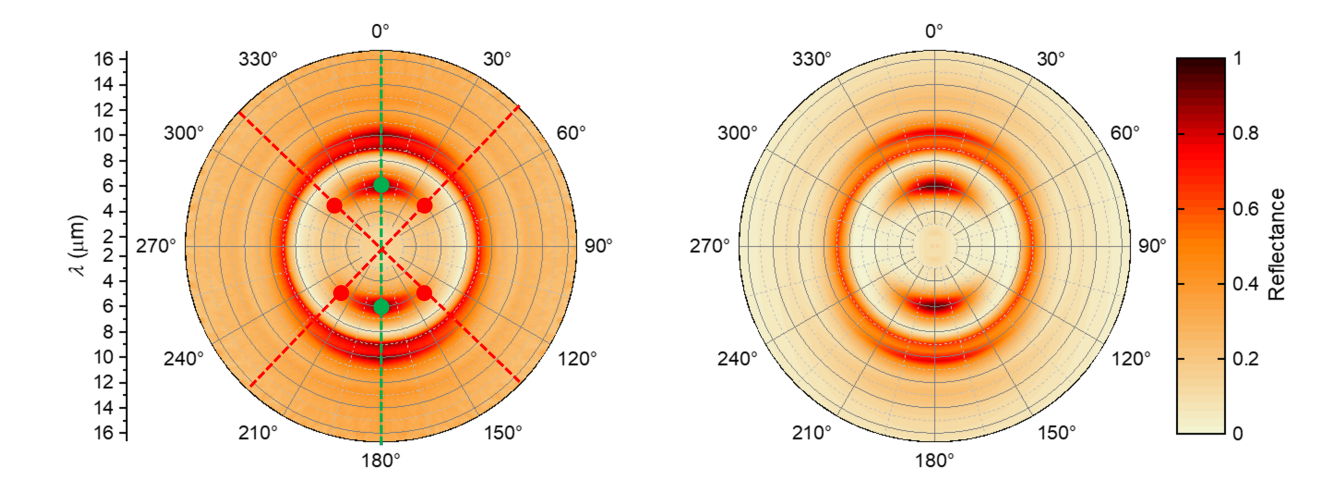


Figure 2. Polar plot of the reflectance of the dipole array as a function of the input polarization. A reflectance maximum appears at 0° and 180° . These angles are marked by a green dot signaling the "on" state of the metasurface. As the orientation of the polarization profile shifts the reflection maximum begins to decrease. At iterations on $45^{\circ} + n \cdot 90^{\circ}$ the metasurface is considered to be in the "off" state marked by a red dot.

pattern is constructed on a $25 \times 25 \times 0.75$ mm³ slide of fused silica. The fused silica substrate is prepared prior to deposition by rinsing with isopropanol-2 and drying with N₂. IP-Dip was used to fabricate a 200 µm thick inverse geometry sacrificial layer. After polymerization the excess monomer is rinsed from the sample using propylene glycol monomethyl ether acetate and isopropanol-2 for two minutes and 5 minutes respectively. Once the excess monomer is removed the sample is allowed to air dry at room temperature for five minutes.⁶

2.3 Metallization and lift-off

After the direct laser writing of the patterned sacrificial layer is completed, the sample was metallized (Kurt J. Lesker PVD 75). Initially, electron-beam evaporation was used to deposit a 7 nm adhesion layer of chromium, sourced from chromium pieces (99.95%) and, immediately following, a 38 nm Au layer (determined experimentally using spectroscopic ellipsometry) evaporated from Au pellets (99.99%). Both films were deposited at a rate of 1 $\rm \mathring{A}/s$. All depositions were carried out at room temperature at a pressure of 2.53 Pa. The substrate holder was rotated during the deposition at approximately 15 rpm to ensure a homogeneous film thickness across the entire sample.⁶

After the metallization, the sacrificial photoresist layer was removed by plasma cleaning at 150 W and a 12 SCCM flow of O_2 (Tergeo Plus, Pie Scientific). After the plasma cleaning, the substrate is completely immersed in acetone until the sacrificial photoresist layer is lifted off completely. Subsequently, the sample is cleaned by rinsing with isopropanol-2 and methanol and dried with N_2 .

3. RESULTS AND DISCUSSION

Linearly polarized reflectance data was captured using a Hyperion 3000 microscope (Bruker) in combination with a Vertex 70 FTIR spectrometer (Bruker) though a $90\times90~\mu\text{m}^2$ square aperture. The reflectance measurements were captured at 11° angle of incidence using a 15x IR Schwarzschild objective with confocal illumination. A mercury cadmium telluride focal plane array detector was used for all measurements. An adjustable, KRS-5, wire-grid polarizer mounted in a custom-built, electro-mechanical, rotation stage was used to polarize the incident radiation.

The results of the hyperspectral imaging can be seen in Fig. 4. The image on the left was taken with an optical microscope to inspect the fidelity of the metasurface post lift-off. Compared to the schematic shown

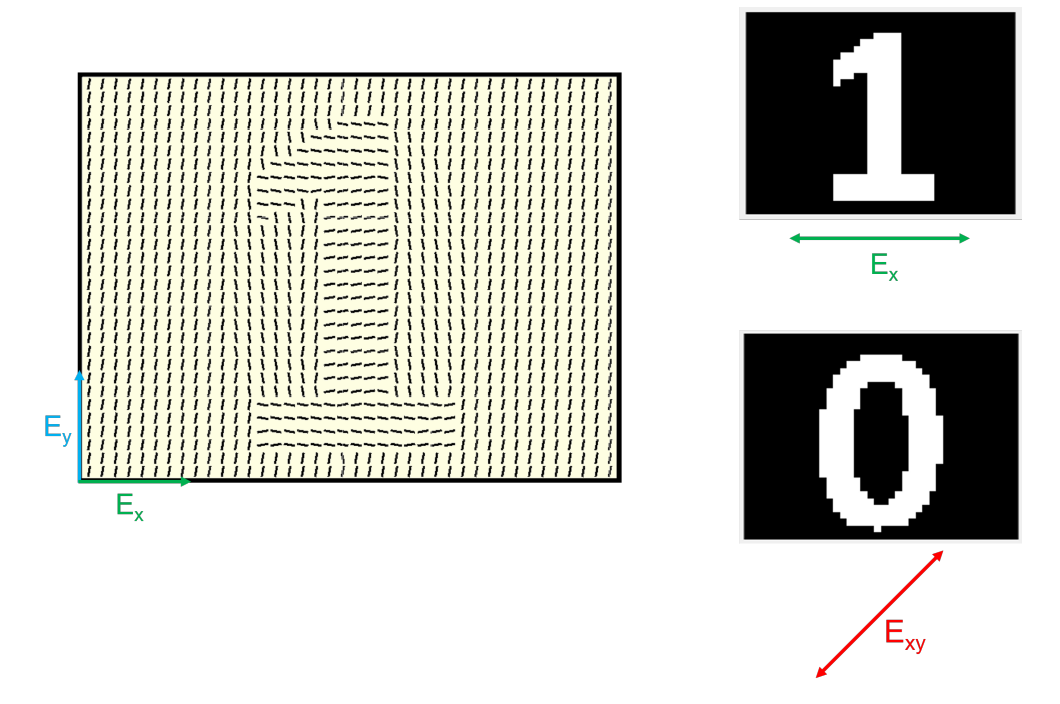


Figure 3. Displays the schematic of the location and orientation of metallic bars for the encoded metasurface. The panels on the right display the image corresponding with the polarization of the incident electric field. When the incident radiation is polarized in \hat{x} the metasurface will appear in the image of a "1." When the incident radiation is polarized in \hat{x} the metasurface results in the image of a "0."

in Fig. 3 a good conformity with the as designed geometry can be observed. The panels to the right of the microscope image depict the hyperspectral images given their corresponding polarizations. When the electric field is polarized in \hat{x} the metasurface displays a "1" and contrarily when polarization is in $\hat{x}y$ the metasurface yields the image of a "0." It can be seen in the polarized reflectance legend that the "1" and "0" reach nearly full reflectance while the surrounding resonators are either much lower, in the case of the "1," or slightly lower, in the case of the "0." This difference in reflectance provides the necessary contrast to observe the definite image. The image is acquired at the wavelength of 6 µm and the vibrational mode of the fused silica substrate does not affect the image quality.

4. CONCLUSION

A plasmonic metasurface was designed and fabricated for the infrared spectral range that allows for the encoding of images. For this particular metasurface two distinct images are encoded, a "1" and a "0." The fabrication of this metasurface uses a three step process, the direct laser writing of an inverse sacrificial layer using two-photon polymerization, a metallization step using electron-beam evaporation, and then the removal of the patterned sacrificial layer using a lift-off procedure. The fabricated metasurface was characterized using hyperspectral imaging to determine the quality of the encoded images. The measurements displayed distinct depictions of the encoded information with sufficient contrast to discern profile and background. This metasurface serves as a proof of concept for applications such as color display, information security, and anti-counterfeiting in the infrared region.

4.1 Acknowledgments

MM, VPS, NS, DL, and TH would like to acknowledge the valuable discussions with sponsors within the NSF IUCRC for Metamaterials. The authors are grateful for support from the National Science Foundation (2052745) within the IUCRC Center for Metamaterials and through the NSF MRI 1828430, the Air Force Research Labs,

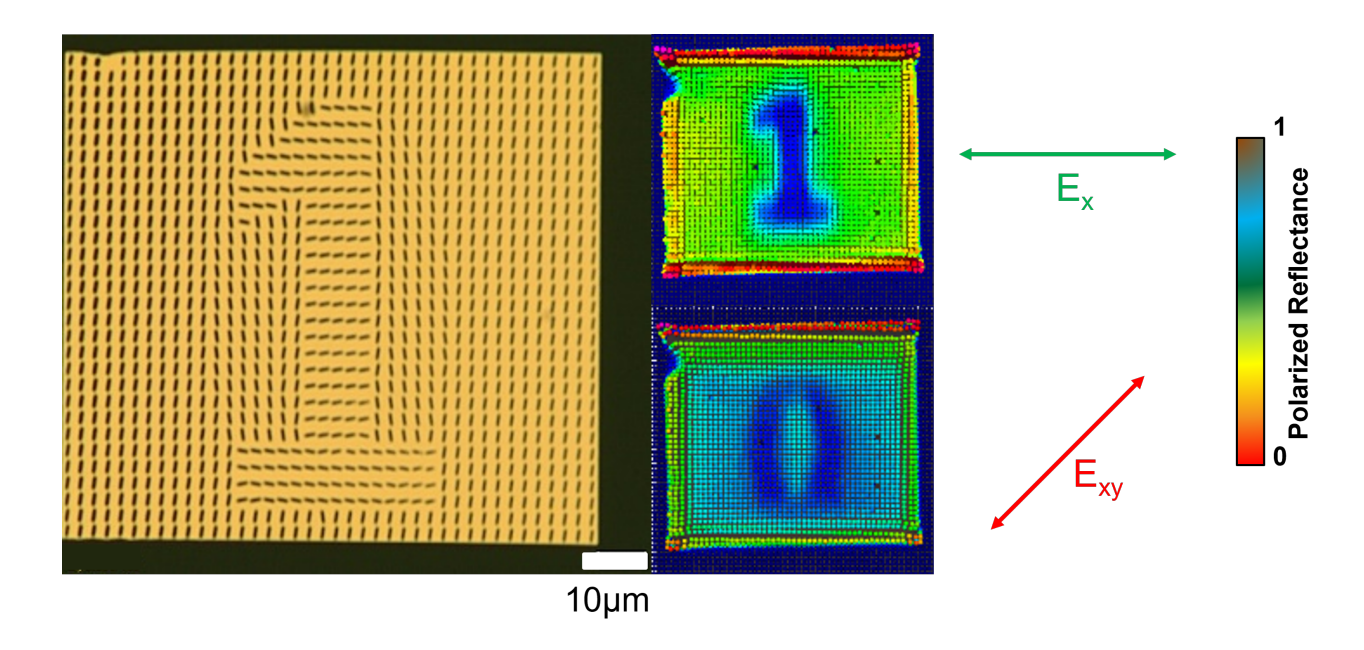


Figure 4. An optical microscope image taken in transmission mode of the metasurface post fabrication to determine the fidelity of the metasurface. The panels to the right of the microscope image depict hyperspectral images obtained at $\lambda = 6 \mu$ m when illuminated with linear polarization in \hat{x} and \hat{x} corresponding to the image of a "1" and "0" respectively.

the J.A. Woollam Foundation, and the Department of Physics and Optical Science of the University of North Carolina at Charlotte.

REFERENCES

- [1] Ding, F., "A review of multifunctional optical gap-surface plasmon metasurfaces," *Pr. Electromagn. Res.* S. 174, 55–73 (2022).
- [2] Tasolamprou, A. C., Skoulas, E., Perrakis, G., Vlahou, M., Viskadourakis, Z., Economou, E. N., Kafesaki, M., Kenanakis, G., and Stratakis, E., "Highly ordered laser imprinted plasmonic metasurfaces for polarization sensitive perfect absorption," *Sci. Rep.-UK* 12, 19769 (2022).
- [3] Dong, F. and Chu, W., "Multichannel-independent information encoding with optical metasurfaces," Adv. Mater. 31, 1804921 (2018).
- [4] Wang, J. and Du, J., "Plasmonic and dielectric metasurfaces: Design fabrication and applications," Appl. Sci. 6, 239 (2016).
- [5] Zang, X., Dong, F., Yue, F., Zhang, C., Xu, L., Song, Z., Chen, M., Chen, P.-Y., Buller, G. S., Zhu, Y., Zhuang, S., Chu, W., Zhang, S., and Chen, X., "Polarization encoded color image embedded in a dielectric metasurface," Adv. Mater. 30, 1707499 (2018).
- [6] McLamb, M., Li, Y., Stinson, P., and Hofmann, T., "Metasurfaces for the infrared spectral range fabricated using two-photon polymerization," *Thin Solid Films* **721**, 138548 (2021).
- [7] McLamb, M., Park, S., V. P, S., Li, Y., Shuchi, N., Boreman, G. D., and Hofmann, T., "Tuning of reciprocal plasmonic metasurface resonances by ultra-thin conformal coatings," *Optics* **3**, 70–78 (2022).
- [8] Luo, J., Smith, N. J., G.Pantano, C., and Kim, S. H., "Complex refractive index of silica, silicate, borosilicate, and boroaluminosilicate glasses analysis of glass network vibration modes with specular-reflection ir spectroscopy," *J. Non-Cryst. Solids* **494**, 94–103 (2018).
- [9] Stinson, V. P., Park, S., M, M., Boreman, G., and Hofmann, T., "Photonic crystals with a defect fabricated by two-photon polymerization for the infrared spectral range," *Optics* 2, 284–291 (2021).